Journal of Alloys and Compounds 509 (2011) 7768–7772

Contents lists available at ScienceDirect

Journal of Alloys and Compounds

journal homepage: www.elsevier.com/locate/jallcom

Synthesis and conductivity of heptadecatungstovanadodiphosphoric heteropoly acid with Dawson structure

Xia Tong [a], Weiming Zhu [a], Qingyin Wu [a,*], Xueyu Qian [a], Zhen Liu [a], Wenfu Yan [b], Jian Gong [c]

[a] Department of Chemistry, Zhejiang University, Hangzhou 310027, PR China
[b] State Key Laboratory of Inorganic Synthesis and Preparative Chemistry, Jilin University, Changchun 130012, PR China
[c] Key Lab of Polyoxometalate Science, the Ministry of Education, Northeast Normal University, Changchun 130024, PR China

ARTICLE INFO

Article history:
Received 8 March 2011
Received in revised form 25 April 2011
Accepted 27 April 2011
Available online 10 May 2011

Keywords:
Heteropoly acid
Dawson structure
Synthesis
Conductivity
Conductive mechanism

ABSTRACT

A new solid high-proton conductor, heptadecatungstovanadodiphosphoric heteropoly acid $H_7P_2W_{17}VO_{62}\cdot 28H_2O$ with Dawson structure was synthesized by the stepwise acidification and the stepwise addition of element solutions. The optimal proportion of component compounds in the synthesis reaction was given. The product was characterized by chemical analysis, potentiometric titration, IR, UV, XRD, ^{31}P NMR, TG-DTA and electrochemical impedance spectroscopy (EIS). The results indicate that $H_7P_2W_{17}VO_{62}\cdot 28H_2O$ possesses the Dawson structure. EIS measurements show a high conductivity (3.10×10^{-2} S cm^{-1} at 26 °C and 75% relative humidity), with an activation energy of 32.23 kJ mol^{-1} for proton conduction. The mechanism of proton conduction for this heteropoly acid is Vehicle mechanism.

1. Introduction

There is considerable current interest in heteropoly acids (HPAs) from both fundamental and practical points of views. They are capable of being fine-tuned at molecular level to promote a variety of applications in catalysis, biomedicine and material science [1–4]. Due to their high proton conductivity, HPAs have also been reported as electrolytes for fuel cells and ultracapacitors. In 1979, Nakamura first reported the high proton conductivity of $H_3PM_{12}O_{40}\cdot 29H_2O$ (M = Mo, W). His work opened up a new field of HPAs as proton conductors.

HPAs are known to show very strong Brønsted acidity. The acid strength of concentrated HPAs aqueous solutions in terms of Hammett acidity function is higher than that of constituent oxoacids and ordinary inorganic acids. The acidity of HPAs solutions is reflected on their proton conductivity which is of the same order of magnitude as that of ordinary mineral acids. HPAs also show high proton conductivity when they are in crystalline forms with determined numbers of water molecules in their structures. There are two types of protons in heteropoly acid crystals: one is the dissociated and hydrated proton that is combined with the HPA anion; the other is the unhydrated proton that is located on the bridge-oxygen in the HPA anion. Because of good mobility of the dissociated protons, HPA crystals have some characteristics of "pseudo liquid". Thus, they are excellent proton conductors, and are promising solid electrolytes [5–8].

To investigate the effect of component elements in HPA on conductivity, we have reported many solid high-proton conducting HPAs such as $H_5GeW_{10}MoVO_{40}\cdot 21H_2O$ [9], $H_6GeW_{10}V_2O_{40}\cdot 22H_2O$ [10] and $H_7[In(H_2O)CoW_{11}O_{39}]\cdot 14H_2O$ [11]. All of them are of Keggin structure and their conductivity is 10^{-4}–10^{-3} S cm^{-1}. Recent studies have shown that as a kind of proton conductors, the conductivity values of heteropoly compounds are closely related to their structures. Herein, we report the synthesis, characterization, conductivity and proton conduction mechanism of heptadecatungstovanadodiphosphoric heteropoly acid $H_7P_2W_{17}VO_{62}\cdot 28H_2O$ ($H_7P_2W_{17}V$) with Dawson structure.

2. Experimental

2.1. Instrument and reagent

Infrared (IR) spectra were recorded on a NICOLET NEXUS 470 FT/IR spectrometer over the wave number range 600–4000 cm^{-1} using KBr pellets. The UV spectrum was measured on a SHIMADZU U-2550 UV-Vis spectrophotometer. X-ray powder diffraction analysis was obtained on a BRUKER D8 ADVANCE X-ray diffractometer using a Cu tube operated at 40 kV and 40 mA in the range of 2θ = 5–40° at a rate of 0.02° s^{-1}. ^{31}P NMR spectrum was recorded in 5 mm outer diameter tubes on a BRUKER MSR-400 spectrometer using 85% H_3PO_4 as the external standard. The thermal stability of the sample was investigated using simultaneous thermogravimetry (TG) and differential thermal analysis (DTA) techniques from room temperature to 600 °C. Measurement was performed using a SHIMADZU thermal analyzer in a Nitrogen stream, with a scanning rate of 10 °C min^{-1}. Impedance measurement of the product was performed on a VMP2 Multichannel potentiostat electrochemical impedance analyzer.

* Corresponding author. Tel.: +86 571 88914042; fax: +86 571 87951895.
E-mail address: qywu@zju.edu.cn (Q. Wu).

0925-8388/$ – see front matter © 2011 Elsevier B.V. All rights reserved.
doi:10.1016/j.jallcom.2011.04.148

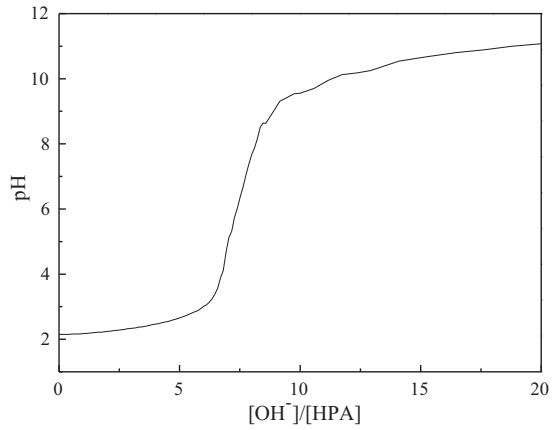

Fig. 1. The potentiometric titration curve of $H_7P_2W_{17}VO_{62}{\cdot}28H_2O$.

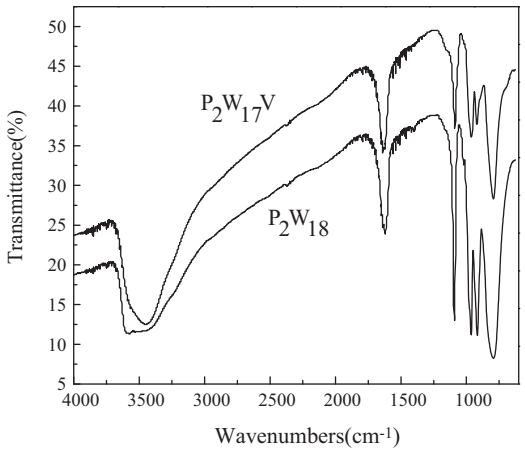

Fig. 2. IR spectra of heteropoly acids with Dawson structure.

All reagents were analysis grade.

2.2. Synthesis of HPA

2.2.1. Synthesis of $[P_2W_{17}O_{61}]^{10-}$

$[P_2W_{18}O_{62}]^{6-}$ (P_2W_{18}) was synthesized according to the literature available [12]. $[P_2W_{17}O_{61}]^{10-}$ (P_2W_{17}) was synthesized by a modification of the method in this literature. 5.0 g $KHCO_3$ was dissolved in 50 mL of water. Then it was added dropwise to 50 mL of aqueous solution containing 20 g P_2W_{18}. The mixture was stirred for an hour to give the white sediment. P_2W_{17} was obtained after being filtrated and dried. Although $K_6P_2W_{18}O_{62}$ is more soluble than $K_{10}P_2W_{17}O_{61}$, it can still precipitate with $K_{10}P_2W_{17}O_{61}$ when treated with potassium bicarbonate. In order to improve the purity of $K_{10}P_2W_{17}O_{61}$, we used sodium bicarbonate instead of potassium bicarbonate.

2.2.2. Synthesis of $H_7P_2W_{17}VO_{62}{\cdot}28H_2O$

0.582 g of $NaVO_3{\cdot}4H_2O$ was dissolved in 6 mL of water and this solution was added dropwise to 84 mL 0.5 mol L^{-1} of hydrochloric acid. The 14 g of presynthesized P_2W_{17} was added to this solution and stirred for an hour. The mixture was extracted with ether in a hydrochloric acid medium. After the ether was removed in the desiccator, orange $H_7P_2W_{17}VO_{62}{\cdot}28H_2O$ was obtained.

2.3. Measurement of conductivity

The product was compressed to a disc under a pressure of 15 MPa at room temperature (26 °C). The diameter was 10 mm and the thickness was 3.64 mm. Two copper sheets were attached to the faces of the disc. Copper slices and copper wires were used as electrodes and lines, respectively. The proton conductivity was measured using a cell: copper |sample| copper.

3. Results and discussion

3.1. Elemental analysis

Phosphorus, tungsten and vanadium were analyzed by ICP; the amount of water was analyzed by thermogravimetry. Found: P = 1.26%, W = 65.12%, V = 1.03%, H_2O = 11.75%.

Calculated for $H_7P_2W_{17}VO_{62}{\cdot}28H_2O$: P = 1.31%, W = 65.92%, V = 1.07%, H_2O = 10.63%.

3.2. Determination of basicity

The number of hydrogens and states of ionization in the HPA can be determined by potentiometric titration [13]. The potentiometric titration curve (Fig. 1) shows that seven protons of $H_7P_2W_{17}VO_{62}{\cdot}28H_2O$ are equivalent and are ionized in the same step.

3.3. IR and UV spectra

The IR spectrum of HPA shows the jump between two vibrational energy levels of the electronic ground state. The vibrations of the oxygen bond reflect the change of mechanical and electronic properties of the bond, and every change has its own characteristic frequency. Vibrations corresponding to the heteropoly acid with Dawson structure appear at 700–1100 cm^{-1}. The vibrational frequencies fall in the sequence of $\nu_{as}(P{-}O_a) > \nu_{as}(M{-}O_d) > \nu_{as}(M{-}O_b{-}M) > \nu_{as}(M{-}O_c{-}M)$, (M = W, V). The vibrational frequencies of $M{-}O_c{-}M$ and $M{-}O_d$ are red shifted, while that of $M{-}O_b{-}M$ is blue shifted, compared with the corresponding vibration frequencies of heteropoly acids with Keggin structure [14].

Fig. 2 shows the IR spectra of $H_7P_2W_{17}V$ and $H_6P_2W_{18}$. The characteristic bands of the heteropoly anions at 700–1100 cm^{-1} are observed, indicating that $H_7P_2W_{17}V$ still maintains Dawson structure after introduction of vanadium atom. The characteristic bands of $P_2W_{17}V$ appear at 1087.5, 963.0, 919.6, and 793.1 cm^{-1}, which correspond to $\nu_{as}(P{-}O_a)$, $\nu_{as}(M{-}O_d)$, $\nu_{as}(M{-}O_b{-}M)$ and $\nu_{as}(M{-}O_c{-}M)$ vibrations, respectively, and the corresponding characteristic bands of P_2W_{18} appear at 1091.4, 963.4, 916.0, and 792.9 cm^{-1}. The difference between the bands of the two compounds probably arises from the substitution of vanadium atom. The bands at about 3450 and 1640 cm^{-1} are assigned to the stretching vibration of O–H bonds and the bending vibration of H–O–H bonds, respectively.

The absorption band of the HPA UV spectrum shows the charge transfer between oxygen and a coordinate metal atom. There is an intense absorption peak at 194 nm ($O_d \rightarrow W$) and a relatively weak absorption peak at 253 nm ($O_b/O_c \rightarrow W$).

3.4. X-ray powder diffraction

X-ray powder diffraction is widely used to study the structural features of HPAs and explain their properties [15]. The data of X-ray powder diffraction are listed in Table 1. Fig. 3 shows the X-ray diffraction pattern of heptadecatungstovanadodiphosphoric heteropoly acid with Dawson structure. The most intense peak exists at about 8.4°. In four ranges of 2θ (i.e. 7–10°, 17–20°, 23–28° and 29–30°), there are characteristic peaks of HPA anions with Dawson structure [16]. Combined with the IR and UV spectra, this confirms that $H_7P_2W_{17}VO_{62}{\cdot}28H_2O$ has Dawson structure.

3.5. ^{31}P NMR spectrum

^{31}P NMR spectroscopy is quite useful for studies of phosphorus chemical environment, which further determine molecular structure of phosphorus-containing compound. The ^{31}P NMR spectrum (Fig. 4) shows that the upfield line ($\delta_2 = -12.04$ ppm) is assigned to the phosphorus atom in the unsubstituted half-anion, while

Table 1
Data of X-ray powder diffraction of $H_7P_2W_{17}VO_{62}\cdot 28H_2O$.

2θ (°)	I/I_0	d (Å)
7.06	0.67	12.52
7.76	0.48	11.39
8.40	1.00	10.53
9.00	0.37	9.83
17.96	0.25	4.94
18.86	0.47	4.71
23.18	0.80	3.84
25.00	0.50	3.56
27.70	0.77	3.22
29.76	0.88	3.00
32.22	0.31	2.78
34.40	0.33	2.61
38.18	0.22	2.36
38.96	0.12	2.31

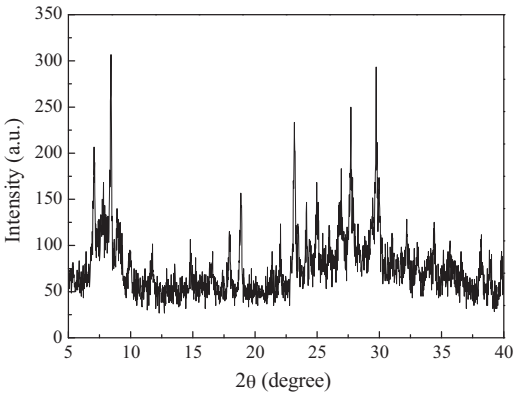

Fig. 3. X-ray diffraction pattern of $H_7P_2W_{17}VO_{62}\cdot 28H_2O$.

downfield chemical shift ($\delta_1 = -10.92$ ppm) corresponds to the phosphorus atom in the substituted half-anion. The downfield shift is attributed to an increase of P–O π bonding when the atom sequence P–O–W is replaced by P–O–V [17]. We conclude that the phosphorus nucleus responsible for the downfield line is undergoing faster relaxation because it is more strongly coupled to the nearby vanadium atom.

3.6. Molecular structure

Fig. 5 shows the polyhedral representation of the molecular structure of heptadecatungstovanadodiphosphoric heteropoly acid with Dawson structure. It is closely related to Keggin structure in that we can imagine that it is constructed from two 9-tungstophosphate fragments of the Keggin anion joined together. There is a heteroatom P at the center of each half which tetrahedrally coordinated to four oxygen atoms, respectively. Each PO_4 tetrahedron is sharing corners with nine WO_6 octahedra. Three

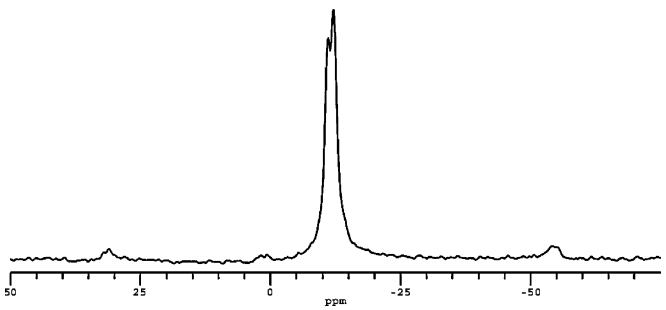

Fig. 4. ^{31}P NMR spectrum of $H_7P_2W_{17}VO_{62}\cdot 28H_2O$.

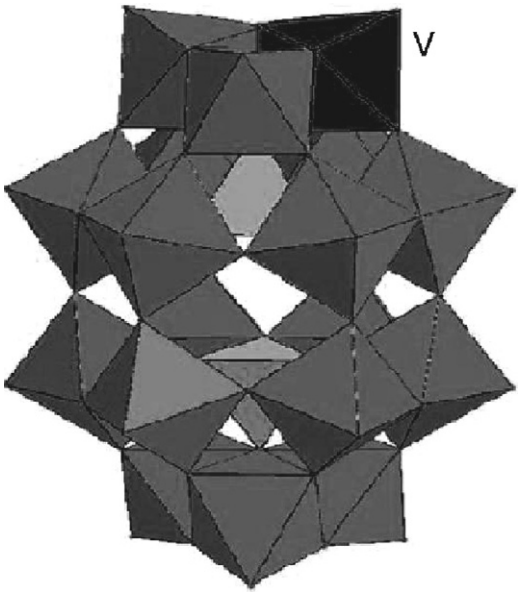

Fig. 5. Polyhederal representation of molecular structure of $H_7P_2W_{17}VO_{62}\cdot 28H_2O$.

WO_6 octahedra form a compact group by sharing edges, while the remaining six octahedra in each of the $[PW_9O_{34}]^{9-}$ fragments form a zigzag ring by alternately sharing edges and corners. The two fragments are linked by six nearly linear W–O–W bonds [18,19]. The HPA with Dawson structure has a rugby ball-like shape. There are two types of tungsten atoms, 6 "polar" and 12 "equatorial". $H_7P_2W_{17}VO_{62}\cdot 28H_2O$ with Dawson structure can be synthesized by the substitution of polar WO_6 octahedra with VO_6 octahedra.

3.7. TG and DTA analysis

Generally speaking, HPAs consist of protons, HPA anions and water. TG and DTA curves of $H_7P_2W_{17}VO_{62}\cdot 28H_2O$ are shown in Fig. 6. The TG curve shows that the total percent of weight loss is 11.75%, indicating that 30.80 water molecules are lost. There are three kinds of water: hydration water, protonized water and structural water. The loss of 23.62 molecules of hydration water happen at first, the second is the loss of 3.73 molecules of protonized water, and 3.45 molecules of structural water are lost at last. Thus, accurate molecular formula of the product is $(H_5O_2^+)_2\cdot H_5[PW_{17}VO_{62}]\cdot 24H_2O$.

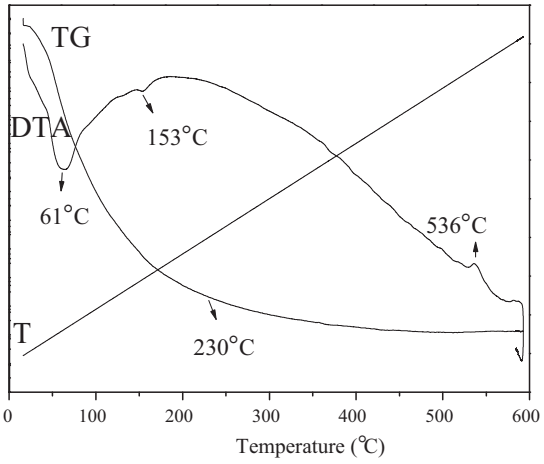

Fig. 6. TG and DTA curves of $H_7P_2W_{17}VO_{62}\cdot 28H_2O$.

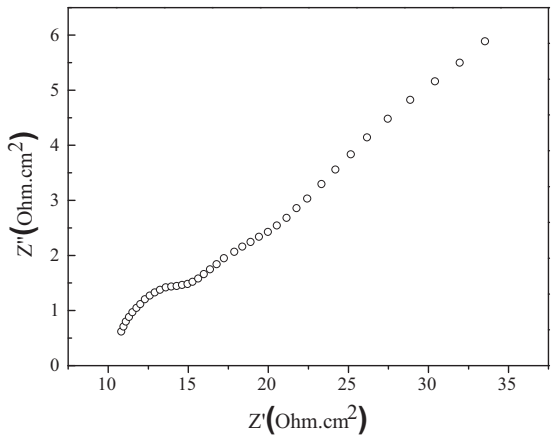

Fig. 7. Electrochemical impedance spectrum of $H_7P_2W_{17}VO_{62}\cdot 28H_2O$.

In general, we take the temperature of the exothermic peak of DTA curve of compound as a way of characterizing its thermostability [20]. In the DTA curve, there are both endothermic and exothermic peaks. The process of dehydration occurring at 61 °C is an endothermic peak. The exothermic peak at 536 °C is due to the decomposition of heteropoly acid $H_7P_2W_{17}VO_{62}\cdot 28H_2O$ with Dawson structure.

3.8. Conductibility

Conductivity is an important parameter. We have recorded the complex impedance spectra of the HPA (over a frequency ranges from 0.01 to 9.99×10^4Hz) at room temperature (Fig. 7). The conductivity can be obtained from these results, as $\sigma = L/(S \times R)$, where R is the resistance, L is the thickness, and S is the area of the tablet [21]. The calculation shows that at room temperature (26 °C) and 75% relative humidity (RH), the conductivity value of the product is 3.10×10^{-2} S cm^{-1}. This compound is a new solid high-proton conducting HPA. Kreuer has suggested that HPA acts as a Bronsted acid toward the hydration water, which is generally loosely bound in the structure, resulting in high proton conductivity [22]. Consequently, the conductivity of HPAs is strictly related to the numbers of water molecules coordinated to the Dawson units.

Fig. 8 shows the Arrhenius plot. From the slope, the activation energy E_a of conductivity can be evaluated using the relation:

$$\sigma = \sigma_0 \exp\left(\frac{-E_a}{\kappa T}\right)$$

where E_a denotes the activation energy of the conductivity, σ_0 is the preexponential factor and κ is the Boltzmann constant. We

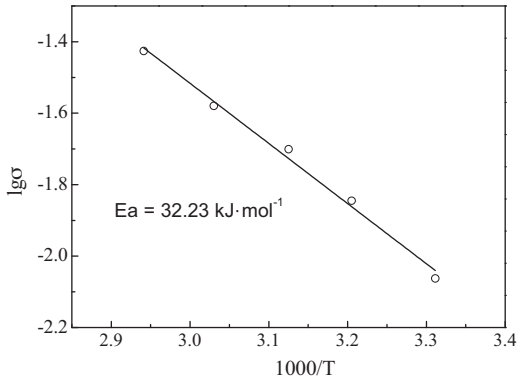

Fig. 8. Arrhenius plot for $H_7P_2W_{17}VO_{62}\cdot 28H_2O$.

can calculate the activation energy of proton conduction, which is 32.23 kJ mol^{-1}. In the range of measured temperature, the conductivity of $H_7P_2W_{17}VO_{62}\cdot 28H_2O$ increases with higher temperature.

The conductivity is a function of the movement of protons. There are two predominant mechanisms of proton conduction: the Vehicle mechanism and the Grotthuss mechanism [23]. In the Vehicle mechanism, water assists proton movement by facilitating transport as H_3O^+ species. This differs from the Grotthuss mechanism, in which a large amount of water can assist proton transport through a hydrogen-bonded network [24]. Generally, the activation energy of the Vehicle mechanism is higher (20 kJ mol^{-1} or more) than that of the Grotthuss mechanism (10 kJ mol^{-1} or less). The activation energy of proton conduction of $H_7P_2W_{17}VO_{62}\cdot 28H_2O$ is 32.23 kJ mol^{-1}, indicating that its mechanism of proton conduction is Vehicle mechanism.

4. Conclusions

$H_7P_2W_{17}VO_{62}\cdot 28H_2O$, a new solid high-proton conducting HPA with Dawson structure was synthesized and characterized by chemical analysis, potentiometric titration, IR, UV, XRD, ^{31}P NMR and TG-DTA. The accurate molecular formula of the product is $(H_5O_2^+)_2\cdot H_5[PW_{17}VO_{62}]\cdot 24H_2O$ and its decomposition temperature is up to 536 °C. Electrochemical impedance spectroscopy measurements show that its conductivity is 3.10×10^{-2} S cm^{-1} at room temperature (26 °C) and 75% RH. The conductivity of $H_7P_2W_{17}VO_{62}\cdot 28H_2O$ increases with higher temperature and the activation energy of proton conduction is 32.23 kJ mol^{-1}, indicating that its mechanism of proton conduction is the Vehicle mechanism. The results also suggest that the $H_7P_2W_{17}VO_{62}\cdot 28H_2O$ performs excellent conductivity bases on the amount of the water in each HPA molecule and the particular Dawson structure.

Acknowledgements

We greatly appreciate the financial support from the National Nature Science Foundation of China (21071124), Nature Science Foundation of Zhejiang Province (Y4090183), the Foundation of State Key Laboratory of Inorganic Synthesis and Preparative Chemistry of Jilin University (2010-16) and the Foundation of Key Lab of Polyoxometalates Science, the Ministry of Education of Northeast Normal University (DS-20080102).

References

[1] T.T. Ali, S.A. Al-Thabaiti, A.O. Alyoubi, M. Mokhtar, J. Alloys Compd. 496 (2010) 553–559.
[2] A.M. Alsalme, P.V. Wiper, Y.Z. Khimyak, E.F. Kozhevnikova, I.V. Kozhevnikov, J. Catal. 276 (2010) 181–189.
[3] S.E. Collins, S.R. Matkovic, A.L. Bonivardi, L.E. Briand, J. Phys. Chem. C 115 (2011) 700–709.
[4] R. Palkovits, K. Tajvidi, A.M. Ruppert, J. Procelewska, Chem. Commun. 47 (2011) 576–578.
[5] H. Gao, Q.F. Tian, K. Lian, Solid State Ionics 181 (2010) 874–876.
[6] G. Lakshminarayana, M. Nogami, Electrochim. Acta 54 (2009) 4731–4740.
[7] L.L. Wang, B.B. Zhou, J.J. Cao, Y.P. Wang, J. Alloys Compd. 432 (2007) 55–60.
[8] H. Gao, K. Lian, Electrochim. Acta 56 (2010) 122–127.
[9] Q.Y. Wu, X.G. Sang, Mater. Res. Bull. 40 (2005) 405–410.
[10] X.G. Sang, Q.Y. Wu, Chem. Lett. 33 (2004) 1518–1519.
[11] Q.Y. Wu, X.G. Sang, F. Shao, W.Q. Pang, Mater. Chem. Phys. 92 (2005) 16–20.
[12] R. Contant, Inorg. Synth. 27 (1990) 104–111.
[13] Q.Y. Wu, X.G. Sang, B. Liu, V.G. Ponomareva, Mater. Lett. 59 (2005) 123–126.
[14] C.N. Kato, K. Hara, A. Hatano, K. Goto, T. Kuribayashi, K. Hayashi, A. Shinohara, Y. Kataoka, W. Mori, K. Nomiya, Eur. J. Inorg. Chem. (2008) 3134–3141.
[15] Q.Y. Wu, S.L. Zhao, J.M. Wang, J.Q. Zhang, J. Solid State Electrochem. 11 (2007) 240–243.
[16] L. Li, Q.Y. Wu, Y.H. Guo, C.W. Hu, Microporous Mesoporous Mater. 87 (2005) 1–9.
[17] S.P. Harmalker, M.A. Leparulo, M.T. Pope, J. Am. Chem. Soc. 105 (1983) 4286–4292.
[18] I.K. Song, M.S. Kaba, M.A. Barteau, Langmuir 18 (2002) 2358–2362.

[19] A. Anzai, K. Inumaru, S. Yamanaka, J. Alloys Compd. 470 (2009) 557–560.
[20] Q.Y. Wu, X.Q. Cai, W.Q. Feng, W.Q. Pang, Thermochim. Acta 428 (2005) 15–18.
[21] S.L. Zhao, Q.Y. Wu, X.L. Huan, L.C. Zhao, J. Appl. Polym. Sci. 107 (2008) 2545–2548.
[22] K.D. Kreuer, Chem. Mater. 8 (1996) 610–641.
[23] K. Checkiewicz, G. Zukowska, W. Wieczorek, Chem. Mater. 13 (2001) 379–384.
[24] M.J. Janik, R.J. Davis, M. Neurock, J. Am. Chem. Soc. 127 (2005) 5238–5245.